

Magnetic properties of the SiO₂(Co)/GaAs interface: Polarized neutron reflectometry and SQUID magnetometry

V. A. Ukleev,¹ N. A. Grigoryeva,² E. A. Dyadkina,¹ A. A. Vorobiev,^{3,1} D. Lott,⁴ L. V. Lutsev,⁵ A. I. Stognij,⁶ N. N. Novitskiy,⁶ A. A. Mistonov,² D. Menzel,⁷ and S. V. Grigoriev^{1,2}

¹*Petersburg Nuclear Physics Institute, Gatchina, 188300 Saint Petersburg, Russia*

²*Faculty of Physics, Saint Petersburg State University, 198504 Saint Petersburg, Russia*

³*European Synchrotron Radiation Facility, F-38000 Grenoble, France*

⁴*Helmholtz-Zentrum Geesthacht, D-21502 Geesthacht, Germany*

⁵*Ioffe Physical Technical Institute of the Russian Academy of Sciences, 194021 Saint Petersburg, Russia*

⁶*Scientific and Practical Materials Research Center of the National Academy of Sciences of Belarus, BY-220072 Minsk, Republic of Belarus*

⁷*Institut für Physik der Kondensierten Materie, Technische Universität Braunschweig, D-38106 Braunschweig, Germany*

(Received 5 June 2012; published 24 October 2012)

The effect of giant injection magnetoresistance (GIMR) was recently observed in a granular SiO₂/(54–75 at. % Co) film on a semiconductor GaAs substrate in a temperature range near $T = 300$ K. The magnetoresistance coefficient reaches a value of $10^5\%$ in a magnetic field of 1.9 T and at a voltage of 90 V. A structural model of the film was proposed based on the results of the grazing-incidence small-angle scattering (GISAXS) and x-ray reflectivity, which showed a specific interface layer 70–75 Å thick separating bulk SiO₂(Co) granular film from the semiconductor substrate. This layer is formed by a monolayer of flattened Co particles which are laterally spaced apart much further than the particles in the bulk film. In the present work, using polarized neutron reflectometry (PNR), we study both the structural and magnetic properties of SiO₂(Co) film separately in the bulk and in the interface layer, which is possible due to the depth resolution of the method. Temperature-dependent PNR and magnetization measurements performed by Superconducting Quantum Interference Device (SQUID) revealed the occurrence of two types of magnetic nanoparticles with different blocking temperatures and magnetization. The magnetization hysteresis curve demonstrated specific two-loop structure in fields 0.5–2 T. Thus our self-consistent results of PNR, GISAXS, and SQUID measurements emphasize the role of the interface features in the SiO₂(Co)/GaAs heterostructures and show a direction for further development of the GIMR theory.

DOI: [10.1103/PhysRevB.86.134424](https://doi.org/10.1103/PhysRevB.86.134424)

PACS number(s): 75.70.Cn, 75.75.-c, 75.50.Lk

I. INTRODUCTION

Efficient spin injection from ferromagnet metal (FM) to a semiconductor (SC) can be obtained in the case of a tunnel barrier for injected electrons at the interface.¹ For that reason, different types of heterostructures with different types of interface barriers were studied during recent years, e.g., the insulator layer between FM and a SC,^{2,3} the diluted magnetic SC layer,⁴ and the Shottky barrier.⁵ If the barrier height is sensitive to an external magnetic field, one can observe positive or negative injection magnetoresistive effects.

The effect of giant injection magnetoresistance (GIMR) was recently observed in SiO₂(Co)/GaAs heterostructures, where the SiO₂(Co) is a thin SiO₂ film with incorporated Co nanoparticles in the concentration range from 54 to 75 at. %.⁶ The injection magnetoresistance phenomenon is magnetic-field-induced suppression of the spin-polarized electron current from the granular film into the semiconductor (GaAs) substrate. The GIMR coefficient reaches $10^5\%$ in a narrow temperature range near $T = 300$ at a magnetic field of $H = 1.9$ T applied in the sample plane and at a voltage $U = 90$ V applied perpendicular to the sample plane. The extreme value of this effect at room temperature and the possibility of controlling the resistivity of the heterostructure by varying the magnetic field are reasons for developing spintronics devices, such as spin injectors, spin diodes, and transistors.⁶

We stress that the described phenomenon has a multiparameter nature and should be theoretically considered in two steps.

First, in the absence of a magnetic field, the inject current flowing from the granular film into the SC shows an exponential growth with an increase of temperature, which is typical for semiconductors. This temperature dependence is complicated by the occurrence of a local maximum of the conductivity close to room temperature ($T = 290$ K). The occurrence of this local maximum is described by the theoretical model of the avalanche process triggered by electrons passing through the potential barrier in the accumulation layer in the SC at the interface, as described in detail in Ref. 6. Secondly, the electron inject current is suppressed by the magnetic field in the order of $H = 1$ T in the narrow temperature range where the local maximum is observed. At temperatures above and below this range (around 290 ± 50 K), the magnetic field does not affect the inject current. Therefore, it is argued in Ref. 6 that the potential barrier is spin-dependent and can be controlled by the magnetic field. This spin-dependent potential barrier is due to the exchange interaction between electrons in the accumulation electron layer in the SC and d electrons of Co. However, the mechanism of the suppression of the current by the magnetic field has not been experimentally clarified yet.

The structural features of the granular films SiO₂(Co)/GaAs were recently studied by grazing incidence small angle x-ray scattering.⁷ In this study, we were able to distinguish a separate interface layer between the granular film and the GaAs substrate. It was shown that the concentration of cobalt nanoparticles at the interface SiO₂(Co)/GaAs is much lower (29 at. %) than that in the bulk of the granular film (77 at. %). Herewith, the distance between granules (320 Å)

is significantly larger at the interface than in the bulk of the granular film (70 Å).⁷ The thickness of this specific interface layer is about 70 Å, which is equal to the size of one granule along the interface normal. This peculiarity of metallic structures assembling on the semiconductor surface is attributed to the physicochemical processes of nucleation, such as sputtering energy and contacting surface tension.⁸ Since two different types of cobalt nanoparticles were discovered in the granular film (nanoparticles located close to each other in the bulk and more separated nanoparticles at the interface), the magnetic properties of the bulk granular film and of the interface layer are expected to be different.

The aim of this work is to investigate the magnetic properties of the SiO₂(Co) ferromagnetic granular film precipitated on a semiconductor substrate at an external magnetic field up to 5 T at different temperatures covering regions with and without the magnetoresistive effect. Depth-resolved magnetization distribution and the field dependence of the magnetization of the films were investigated by polarized neutron reflectometry (PNR). Integral magnetic properties of the samples were studied by Superconducting Quantum Interference Device (SQUID) magnetometry.

The present paper is organized in the following way. Section II describes the samples under investigation. Section III gives the results of polarized neutron reflectometry experiments (Sec. III A and SQUID measurements (Sec. III B) along with some discussion. Section IV contains concluding remarks.

II. SAMPLES

Granular films SiO₂ (*x* at. % Co) were prepared by ion beam cosputtering of the composite cobalt-quartz targets on the commercial (100)-oriented *n*-GaAs substrates with a thickness of 0.4 mm and a carrier concentration of 10¹⁵ cm⁻³. All peculiarities of the sputtering method and choice of components are described in Ref. 9. The concentrations of the Co nanoparticles in SiO₂ were controlled by the relation between the areas of cobalt and quartz targets. The thicknesses of the investigated granular films were controlled by the time of deposition of Co and SiO₂ with a given deposition rate in the process of synthesis of the samples. We investigated two heterostructures with different nominal thicknesses of the granular films: 400 Å for PNR measurements and 900 Å for SQUID. Samples were covered by a capping gold layer with a thickness about 20 Å, which was used as a conductive contact for GIMR measurements.

III. EXPERIMENT

A. Polarized neutron reflectometry

PNR was used to study the magnetic and nuclear in-depth profiles of the Au/SiO₂ (75 at. % Co)/GaAs sample with a nominal thickness of 400 Å. Typical geometry of the polarized neutron reflectometry experiment is shown in Fig. 1. In the case of specular reflectometry, the angle α_f of the scattered beam with wave vector \mathbf{k}_f is equal to the angle of incidence α_i of the primary beam with wave vector \mathbf{k}_i . Since only those neutrons which were reflected under specular angles were detected, the lateral components of neutron momentum transfer Q_x and Q_y

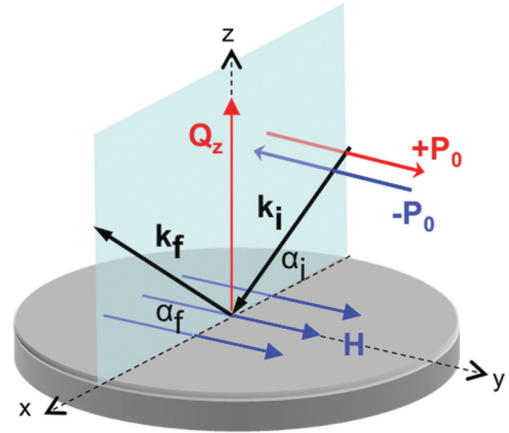


FIG. 1. (Color online) Typical geometry of the polarized neutron reflectometry experiment.

are equal to zero, and the vertical component Q_z is expressed by the equation

$$Q_z = \frac{4\pi}{\lambda} \sin(\alpha_f), \quad (1)$$

where λ is the neutron wavelength.¹⁰

The experiments were carried out at the reflectometer for polarized neutrons at the FRG research reactor (GKSS Forschungszentrum, Germany) which exploited a neutron beam with $\lambda = 6.35$ Å ($\delta\lambda/\lambda = 0.05$) and the initial polarization $P_0 = 0.95$. Scattered neutrons were detected by the position-sensitive detector at 256×256 pixels. The intensities of the reflected beams with initial polarization $+\mathbf{P}_0$ and $-\mathbf{P}_0$, i.e., along with and opposite to the direction of the external magnetic field \mathbf{H} , were measured one by one. A magnetic field from 0 to 0.24 T was applied perpendicular to \mathbf{k}_i and parallel to the film surface. The direction of \mathbf{P}_0 with respect to \mathbf{H} was switched by a spin-flipper.

Measurements were performed at two temperatures: $T = 300$ K (where the GIMR effect reaches maximum) and $T = 120$ K (where the GIMR effect is not detected). The data for every temperature were taken after the demagnetization process. In both cases, no difference between reflectivity curves $I(+\mathbf{P}_0)$ and $I(-\mathbf{P}_0)$ was observed at $H = 0$ mT, while applying the external field resulted in a pronounced splitting of two components (Fig. 2).

The Parratt method was used for an evaluation of the experimental data.¹¹ The model, which fits the experimental data in the best way, consists of four layers on a GaAs substrate: the capping Au layer, and the top, middle, and bottom (sub)layers of the granular film [(GF1), (GF2), (GF3), and GaAs substrate]. Every layer is characterized by four parameters: thickness (d), roughness (σ), and nuclear and magnetic scattering length densities (SLD) N_n and N_m , respectively. The latter has the opposite sign for neutrons with $+\mathbf{P}_0$ and $-\mathbf{P}_0$ and its value is directly proportional to the magnetization component \mathbf{M} parallel to \mathbf{H} :

$$M = \frac{2\pi\hbar^2}{m_n\mu_n} \frac{N_m}{4\pi} \approx 3.44 \times 10^8 N_m, \quad (2)$$

where m_n is the neutron mass and μ_n is the neutron magnetic moment. Thus the SLD profile represents the distribution

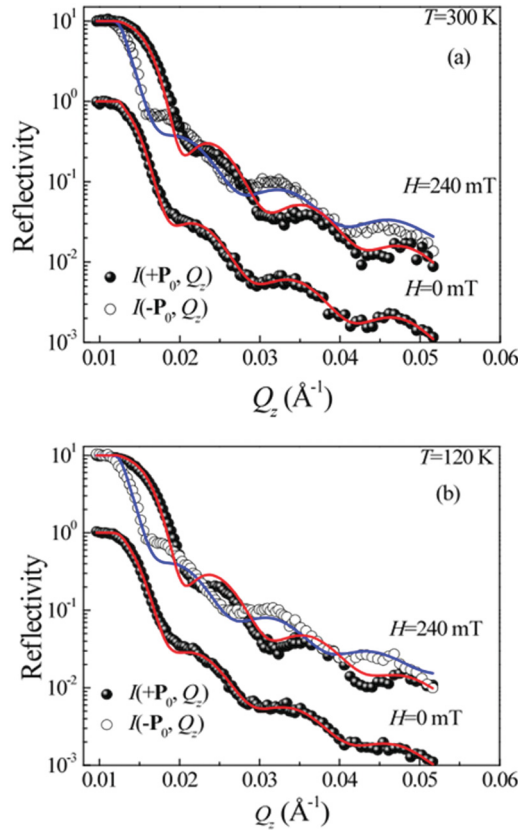


FIG. 2. (Color online) The experimental (symbols) and fitted model (lines) reflectivity curves for the sample Au/SiO₂ (75 at. % Co)/GaAs at fields $H = 0$ and 240 mT and at temperatures (a) $T = 300$ K and (b) $T = 120$ K. Experimental and model curves at $H = 240$ mT are multiplied by 10 for convenience.

of the scattering potential of the sample in the z direction. Comparing SLD profiles $\rho^+ = N_n + N_m$ and $\rho^- = N_n - N_m$ corresponding to $R(+\mathbf{P}_0)$ and $R(-\mathbf{P}_0)$, respectively, one can obtain a value of the magnetization in every layer forming the sample film. Models with smooth interfaces ($\sigma = 0$) between layers were used to fit the experimental data and thickness, and SLD parameters were varied in the fit procedure.

As an example, the profile with parameters obtained from the fit of Au/SiO₂ (75 at. % Co)/GaAs at $T = 300$ K is presented in Fig. 3. From a splitting of ρ^+ and ρ^- , one can conclude that only the GF2 and GF3 layers are magnetized under applied field $H = 0.24$ T and that the magnetization value is higher in GF2. The GF1 layer remains nonmagnetic because, as we suggest, it consists of fully oxidized cobalt nanoparticles which show paramagnetic behavior at room temperature.

Consequently, the present PNR investigation not only confirms the existence of the specific interface layer (GF3 in our notation) previously found by GISAXS and x-ray reflectivity,⁷ but it allows one to study its magnetic properties. We note that the thickness of the GF3 layer [(61 ± 5) Å] obtained from the PNR fit is in good agreement with the value found from x-ray reflectometry.⁷

Magnetization of GF2 and GF3 calculated from N_m according to Eq. (2) is presented in Fig. 4 as a function of an applied field at different temperatures. Magnetization of both layers

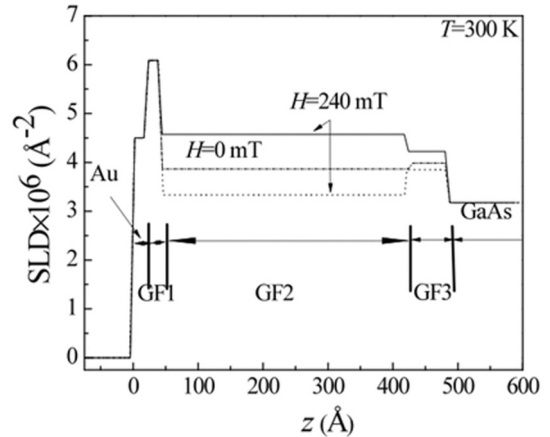


FIG. 3. The SLD profiles ρ^+ (solid line) and ρ^- (dashed line) of the sample Au/SiO₂ (75 at. % Co)/GaAs at $H = 0.24$ T and $T = 300$ K. The dot-dashed line corresponds to the SLD profile in $H = 0$ T for every polarization of neutrons.

increases with an applied field. Cooling the sample to $T = 120$ K leads to a more rapid increment of magnetization. One can see that the increment of magnetization of the bulk layer GF2 at $T = 300$ K is similar to that at $T = 120$ K. Moreover, in the field of $H = 240$ mT, magnetization saturates. Compared to bulk cobalt, the saturation magnetization of the GF2 layer is about five times smaller. Magnetization of the interface layer GF3 at $T = 120$ K is two times larger than at $T = 300$ K and does not saturate up to $H = 240$ mT. For further research of magnetic properties, SQUID magnetometry were used.

B. SQUID

Magnetometry measurements were carried out with the SQUID-magnetometer Quantum Design MPMS-5S at the Institute of Condensed Matter Physics, Braunschweig, Germany. The heterostructure Au/SiO₂ (75 at. % Co)/GaAs with a thickness of 900 Å was studied. Magnetization curves $M(H)$ at $T = 5, 250, 300,$ and 350 K were taken. The field dependence of magnetization is almost the same at $T = 250,$

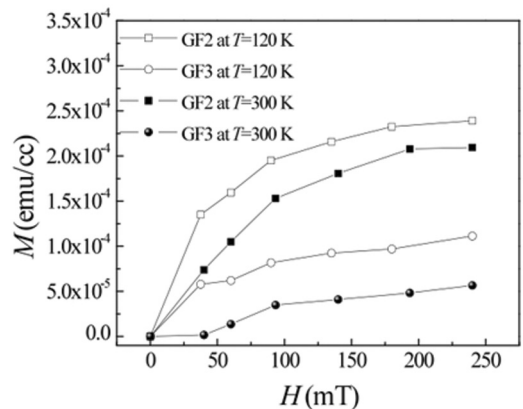


FIG. 4. Magnetic field dependences of magnetization obtained from PNR data according to Eq. (2) for layers GF2 and GF3 of the sample Au/SiO₂ (75 at. % Co)/GaAs. Open squares, GF2 at $T = 120$ K; filled squares, GF2 at $T = 300$ K; open circles, GF3 at $T = 120$ K; filled circles, GF3 at $T = 300$ K.

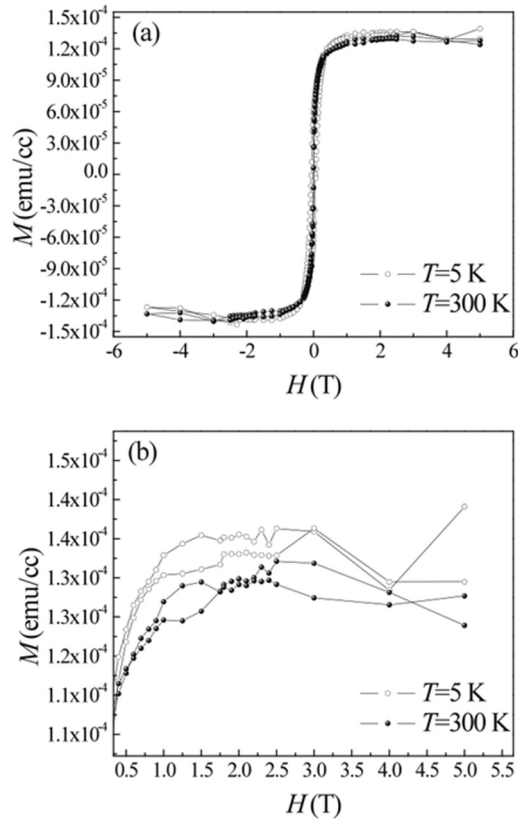


FIG. 5. (a) Magnetic field dependence of the Au/SiO₂ (75 at. % Co)/GaAs sample magnetization at $T = 5$ and 300 K measured by SQUID. (b) Scaled hysteresis “pocket” loops.

300, and 350 K, so only representative measurements at $T = 5$ and 300 K are shown in Fig. 5(a) after subtraction of the diamagnetic contribution of the GaAs substrate and the SiO₂ matrix. Magnetic field was applied parallel to the plane of the film. At $T = 120, 300,$ and 350 K, the sample demonstrates typical superparamagnetic behavior in a range of magnetic fields $0 < H < 0.3$ T. Further enhancement of the applied field induces an appearance of specific hysteresis loops, so-called “pockets,” which are zoomed in Fig. 5(b). Previously these loops were also observed in SiO₂(Co)/GaAs.¹² At $T = 5$ K, a hysteresis loop with a coercivity field $H_c = 0.11$ mT can be observed.

Additionally, we measured the temperature dependence of the magnetization $M(T)$ using field-cooling (FC) and zero-field-cooling (ZFC) modes. The FC mode implies an application of constant magnetic field $H = 0.01$ T to the sample kept at a temperature far above a certain characteristic blocking temperature T_b and cooling the sample in this field to $T \ll T_b$ while recording the magnetization. The ZFC mode consists of the following sequential steps: cooling the sample in zero field to $T \ll T_b$, applying field $H = 0.01$ T, and heating the sample to $T \gg T_b$ while measuring M .

Figure 6(a) shows FC and ZFC curves of magnetization for the sample Au/SiO₂ (75 at. % Co)/GaAs) 900 Å in the applied field $H = 10$ mT. Below T_b , nanoparticles in the granular film show a blocked behavior, which is typical for heterogeneous nanoparticles systems.¹³ For low temperatures ($T < T_b$), a highly irreversible metastable frozen state may occur. A small

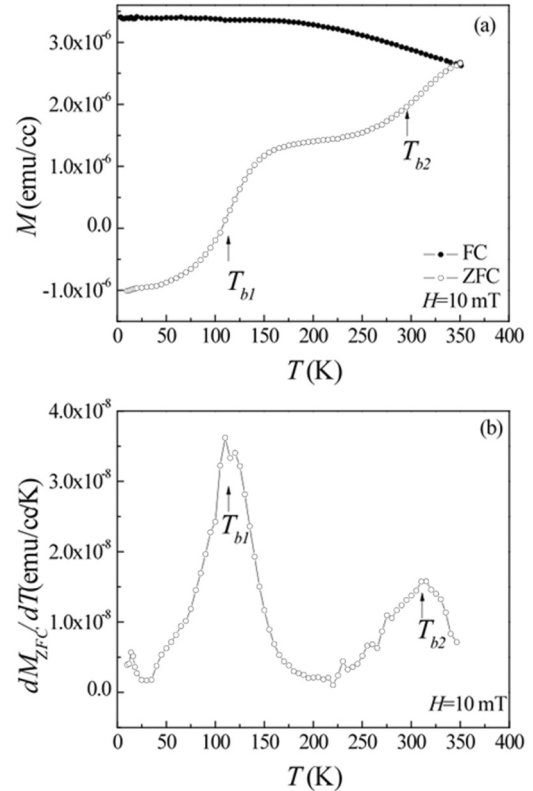


FIG. 6. (a) FC/ZFC curves of magnetization and (b) first derivative of $M(H)$ ZFC curves of magnetization of the Au/SiO₂ (75 at. % Co)/GaAs sample in applied field $H = 10$ mT.

field applied in FC mode creates a relatively stable state with most of the moments of the nanoparticles directed along the field, summed in a relatively high magnetization which increases with cooling. In ZFC mode, the magnetic system is frozen in one of many possible configurations (metastable state) created due to magnetic interactions between nanoparticles. An applied small magnetic field cannot force the frozen moments to rotate to the field direction. Thus, magnetization remains small at low temperature and increases upon a temperature increase. The ZFC curve has a peak-type character due to the concurrence between thermal energy and interactions of the particle with the field and with the neighbors. The difference between ZFC and FC magnetization indicates that the system has a number of metastable states below T_b .¹⁴ The blocking temperature of a superparamagnetic system was found to be an inflection point of the magnetization curve $M_{ZFC}(T)$ (Ref. 15) [as an extremum of the dM_{ZFC}/dT in Fig. 6(b)]. The ZFC curve of the sample Au/SiO₂ (75 at. % Co)/GaAs has two inflection points [Fig. 6(a)], which indicates the existence of two different superparamagnetic systems with different blocking temperatures T_{b1} and T_{b2} presented in the film.

Measurements in FC/ZFC modes at different applied fields H from 10 to 150 mT were performed. As it was found, with an increase of applied magnetic field, blocking temperatures shift rapidly to the low-temperature region (Fig. 7), which is typical for superparamagnets.¹⁶ The linear extrapolation of the blocking temperatures T_{b1} and T_{b2} in the range of small fields gives the values $T_{b1}(0) = 177$ K and $T_{b2}(0) = 444$ K.

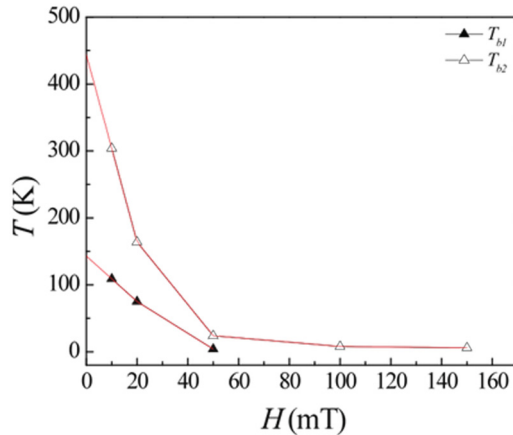


FIG. 7. (Color online) Blocking temperature over applied field H dependence for sample Au/SiO₂ (75 at. % Co)/GaAs. Lines denote the extrapolation.

We suggest that the presence of two blocking temperatures for the sample is caused by two types of magnetic nanoparticles, i.e., at the interface and in the bulk of the granular film, as found in Ref. 7. Indeed, the blocking temperature can be expressed in terms of the magnetic interactions between nanoparticles as well as Curie temperature.¹⁷ In the self-consistent field (Weiss field) approach, the blocking temperature is

$$T_b = \frac{\langle S \rangle^2 n J}{3k_B}, \quad (3)$$

where $\langle S \rangle$ is the average magnetic moment of the nanoparticle, J is the interaction between nanoparticles, n is the number of nearest neighbors, and k_B is the Boltzmann constant.

It is easy to estimate the mean Co nanoparticle size using cobalt concentration and the interparticle distance. According to Ref. 7, the distance between cobalt nanoparticles in the interface layer is about $l = 320$ Å, while in the bulk layer it is $l = 70$ Å. Mean particle size can be calculated using the formula¹⁸

$$d \approx \left(\frac{6x_v}{\pi} \right)^{1/3} l, \quad (4)$$

where d denotes the diameter of the spherical nanoparticle, x_v is the volume fraction, and l is the average interparticle distance. Calculation gives an average nanoparticle size $d_b = 80$ Å for 75 at. % of Co and $d_i = 280$ Å for 29 at. % of Co. A model of the film layers is presented in Fig. 8. It is also possible to estimate the blocking temperature relation of bulk and interface layer nanoparticles using the formula from Eq. (3) with the assumption of only dipole-dipole interaction between the nanoparticles. The estimation results is $T_{b1}/T_{b2} \approx 0.41$, while the experimental relation is $T_{b1}/T_{b2} \approx 0.39$. This is because bulk layer nanoparticles due to the high concentration have some ferromagnetic exchange as well as dipole-dipole interaction,¹² and because of the nonspherical shape of the nanoparticle at the interface, which leads to additional anisotropy.

The magnetization curve shown in Fig. 5 demonstrates features that can be attributed to two different magnetic systems in the granular film. The nanoparticles in the granular

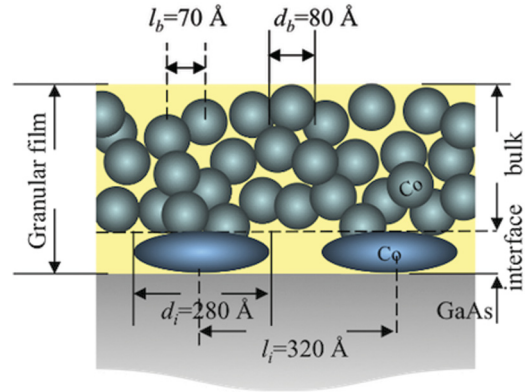


FIG. 8. (Color online) A model of nanoparticles assembling in SiO₂ (75 at. % Co) granular film on GaAs substrate.

film with the characteristic interparticle distance of 70 Å are magnetized in the region of relatively low fields, $0 < H < 0.5$ T. It must be noted that the saturation fields of the layer GF2 are an order of magnitude smaller than the fields where the GIMR effect takes place. Therefore, one has to find a different magnetic layer, which should have magnetic changes in the field ranging from $H = 1$ to 2 T. It is the layer of the nanoparticles at the interface to which we ascribe the hysteretic behavior within the range from $H = 0.8$ to 2 T (hysteresis loop pockets in Fig. 5). Such pockets near the saturation field indicate the existence of magnetic moments that slanted easy magnetization axes. This was also observed in quantum-dot magnetic nanodisks,^{19,20} magnetic microwires,²¹ and exchange biased systems.^{22–27} However, the magnetization mechanism in these structures cannot be applied to the present experimental results due to the single-domain formation of cobalt nanoparticles in our samples.

The assumption of the interface origin of magnetization loop pockets is also supported by the layer-resolved magnetization presented in Sec. III A (Fig. 4). Two contributions to the magnetization are taken into account—from the thick layer of the relatively small grains (GF2) and from the thin interface layer of the relatively large grains (GF3). The former is responsible for the nonhysteretic increase of the magnetization upon increase of the magnetic field. The latter gives rise to the relatively small hysteresis loop that appeared on the top of the saturated magnetization curve. The relative values of both contributions can be calculated from the magnetization found in the reflectometry measurements; they are equal to the product of the layer's magnetization and their thickness. The ratio of the two contributions estimated from the reflectometry measurements corresponds to the measured values taken from the SQUID measurements.

Two more comments can be made concerning the interface layer. First, it is supposed that the thickness of the layer GF3 is defined only by the physicochemical processes going in sputtered Co and quartz interacting between each other and with the GaAs substrate on the very first step of the sample formation. This means that the thickness of the interface layer is independent of the whole thickness of the granular film and that the magnetic contribution of the interface nanoparticles to the integral magnetization is the same for all samples of this type. At the same time, the contribution of the bulk layer GF2

is obviously proportional to its thickness, which can be easily changed through the process of synthesis.

Secondly, the additional hysteresis pockets are antisymmetrically observed upon the negative and positive change of the applied magnetic field. In other words, the magnetization of the interface layer is not saturated up to field values of about 1.5–2 T, and it remains saturated upon a decrease of the field down to zero only. This means that the saturated magnetization of the interface layer disappears together with the magnetization of the thick layer GF2. This observation led us to the speculation that the interface layer GF3 can be ferromagnetically coupled (through Heisenberg interaction) to the granular film itself (GF2) and antiferromagnetically coupled (through RKKY interaction) to the polarized electrons accumulating in the semiconductor GaAs. However, this speculation should be experimentally proven.

IV. CONCLUSION

In the present work, using polarized neutron reflectivity, we study both the structural and magnetic properties of

SiO₂(Co) film separately in the bulk and in the interface layer, which is possible due to the depth resolution of the method. Temperature-dependent PNR and magnetization measurements performed by SQUID unambiguously showed the occurrence of two types of magnetic nanoparticles with different blocking temperatures and magnetization. The magnetization hysteresis curve demonstrated specific two-loop structure in fields 0.5–2 T. Thus our self-consistent results of PNR, GISAXS, and SQUID measurements emphasize the role of the interface features in the SiO₂(Co)/GaAs heterostructures and show a direction for further development of the GIMR theory.^{25–32}

ACKNOWLEDGMENTS

This work was performed within the framework of a Federal Special Scientific and Technical Program (Projects No. 02.740.11.0874 and No. 07.514.12.4003), the Russian Foundation for Basic Research, Grants No. 10-02-00516 and No. 12-02-12066-ofi_m, and by the Ministry of Education and Science of the Russian Federation, Project No. 2011-1.3-513-067-006.

-
- ¹X. Lou, C. Adelman, M. Furis, S. A. Crooker, C. J. Palmström, and P. A. Crowell, *Phys. Rev. Lett.* **96**, 176603 (2006).
²A. M. Bratkovsky, *Phys. Rev. B* **56**, 2344 (1997).
³M. N. Baibich, J. M. Broto, A. Fert, F. Nguyen Van Dau, F. Petroff, P. Etienne, G. Creuzet, A. Friederich, and J. Chazelas, *Phys. Rev. Lett.* **61**, 2472 (1988).
⁴G. Schmidt, G. Richter, P. Grabs, C. Gould, D. Ferrand, and L. W. Molenkamp, *Phys. Rev. Lett.* **87**, 227203 (2001).
⁵V. V. Osipov and A. M. Bratkovsky, *Phys. Rev. B* **72**, 115322 (2005).
⁶L. V. Lutsev, A. I. Stognij, and N. N. Novitskii, *Phys. Rev. B* **80**, 184423 (2009).
⁷N. Grigor'eva, A. Vorob'ev, V. Ukleev, E. Dyad'kina, L. Lutsev, A. Stognij, N. Novitskii, and S. Grigor'ev, *JETP Lett.* **92**, 767 (2010).
⁸H. W. Chang, J. S. Tsay, Y. C. Hung, F. T. Yuan, W. Y. Chan, W. B. Su, C. S. Chang, and Y. D. Yao, *J. Appl. Phys.* **101** 09D124 (2007).
⁹A. I. Stognij, N. N. Novitskii, and O. M. Stukalov, *Tech. Phys. Lett.* **29**, 43 (2003).
¹⁰X.-L. Zhou and S.-H. Chen, *Phys. Rep.* **257**, 223 (1995).
¹¹L. G. Parratt, *Phys. Rev.* **95**, 359 (1954).
¹²A. A. Stashkevich, Y. Roussigné, P. Djemia, D. Billet, A. I. Stognij, N. N. Novitskii, G. Wurtz, A. Zayats, G. Viau, G. Chaboussant, F. Ott, L. V. Lutsev, and Belotelov, *J. Appl. Phys.* **104**, 093912 (2008).
¹³E. C. Stoner and E. P. Wohlfarth, *Philos. Trans. R. Soc. London, Ser. A* **240**, 599 (1948).
¹⁴Y. Zhu (Ed.), *Modern Techniques for Characterizing Magnetic Materials* (Springer, New York, 2005), pp. 107–155.
¹⁵T. Song and R. M. Roshko, *Physica B* **275**, 24 (2000).
¹⁶W. F. Brown, Jr., *Phys. Rev.* **130**, 1677 (1963).
¹⁷G. S. Krinchik, *The Physics of Magnetic Phenomena* (Moscow State University Press, Moscow, 1985) (in Russian).
¹⁸C. L. Chien, *Annu. Rev. Mater. Res.* **25**, 129 (1995).
¹⁹M. Kostylev, R. Magaraggia, F. Y. Ogrin, E. Sirotkin, V. F. Mescheryakov, N. Ross, and R. L. Stamps, *IEEE Trans. Magn.* **44**, 2741 (2008).
²⁰Y. P. Ivanov, K. V. Nefedev, A. I. Iljin, E. V. Pustovalov, and L. A. Chebotkevich, *J. Phys.: Conf. Ser.* **266**, 012117 (2011).
²¹V. V. Rodionova, Ph.D. thesis, Moscow State University, 2010.
²²A. N. Dobrynin, and D. Givord, *Phys. Rev. B* **85**, 014413 (2012).
²³B. Kalska, P. Fumagalli, M. Hilgendorff, and M. Giersig, *Mater. Chem. Phys.* **112**, 1129 (2008).
²⁴Y. X. Wang, N. N. Yang, M. B. Wei, Y. J. Zhang, H. B. Liu, Y. Liu, and J. H. Yang, *J. Alloys Compd.* **509**, 6626 (2011).
²⁵J. Noguees, V. Skumryev, J. Sort, S. Stoyanov, and D. Givord, *Phys. Rev. Lett.* **97**, 157203 (2006).
²⁶A. N. Dobrynin, D. N. Ievlev, C. Hendrich, K. Temst, P. Lievens, U. Hörmann, J. Verbeeck, G. Van Tendeloo, and A. Vantomme, *Phys. Rev. B* **73**, 245416 (2006).
²⁷A. N. Dobrynin, K. Temst, P. Lievens, J. Margueritat, J. Gonzalo, C. N. Afonso, E. Piscopiello, and G. Van Tendeloo, *J. Appl. Phys.* **101**, 113913 (2007).